Cautionary Tales of Persistent Accumulation of Numerical Error: Dispersive Centered Advection

Matthew W. Hecht

Computational Physics and Methods, CCS Division, Los Alamos National Laboratory
Mail Stop B296, Los Alamos, NM, 87545, USA.

Abstract

In ocean modelling there is widespread appreciation for the severity of any error which involves spurious diapycnal mixing. Indeed, the extreme disparity between the timescales which characterize mixing in the isopycnal and diapycnal directions is a defining feature of oceanic fluid dynamics. Particular concern is therefore raised by any source of spurious diapycnal mixing which is persistent, capable of acting with unchanging sign over the very long timescales associated with oceanic adjustment. Here, in a simplified problem in which the impact of such a persistent error may be more readily diagnosed, we identify a potentially severe source of cooling within and below the thermocline of ocean climate models.

Keywords: advection, dispersive error, diapycnal mixing, convection, ocean modelling

1. Introduction

Ocean modelling is fundamentally based upon numerical approximation to continuous equations describing fluid flow, and so numerical error, in the sense of departure from an exact continuum form, is inescapable. Some errors are of course more damaging than others. If an error tends persistently toward a certain sign or effect then it will, over time, accumulate to produce an ever larger bias. One would prefer to minimize any source of error, but judgement is required in the choice of which errors to address most aggressively. This judgement rests not only on a quantitative evaluation of error measures, but should also be based upon insight regarding the qualitative impact of the numerical error in question.

Qualitatively speaking, errors which contribute to cross-isopycnal mixing are especially important to reduce. Working within a Z-coordinate ocean model, sometimes referred to as a Bryan-Cox-Semtner model, we use an isopycnal tracer mixing scheme to reduce the cross-isopycnal error that can so greatly compromise an ocean model, a choice nearly always made in the ocean component of climate models today. In this paper we consider the interplay between two numerical schemes, one being the lateral tracer mixing scheme, the other being the tracer advection scheme. We find that the tracer mixing scheme allows for an error to go unchecked, but it is the advection scheme that is the source of the error in question.

The original ocean model of Bryan (1969) used a second-order centered-in-space and leapfrog centered-in-time discretization. Alternative temporal discretizations have sometimes been adopted in descendants of that model (see for instance the two-time-level implementation described in Griffies et al. (2004) and Griffies (2004), and Hecht (2006) for an overview of forward-in-time methods in ocean modelling), and alternatives to centered-in-space tracer advection are widely available, including those of Gerdes et al. (1991), Holland et al. (1998) and Adcroft et al. (2005), yet centered leapfrog discretizations remain in common use.

One explanation for the longevity of the original centered-in-space and leapfrog-in-time approach is the efficiency of the discretization. Cost alone is not, however, the sole issue. The leading-order discretization error of alternative advection schemes is most often dissipative in character, as contrasted with the dispersive leading error of the centered-in-space scheme. Dispersive error tends to produce grid-scale noise, or oscillations, whereas dissipative error produces excessive smoothing (see Hecht et al. (1995), Hecht et al. (2000) for illustration). Concerns with the introduction of spurious dissipation persist. Ocean modelers tend to be particularly reticent to introduce spurious cross-frontal mixing, so as not to short-circuit the large-scale heat transport of the oceans through the Veronis Effect (Veronis (1975)).

A notable effort to quantify the level of implicit dissipation associated with the advection scheme was presented in Griffies et al. (2000). Even with this quantitative assessment of the numerical error, the qualitative impact of the dissipative error raises concerns, as in a recent effort to use a quasi-monotonic advection scheme within a global 0.1° version of the Los Alamos Parallel Ocean Program (POP, as described in Maltrud et al. (2010) and references within; the advection scheme was developed by K. Lindsay (private communication)). The jets of the equatorial Pacific were not as well represented as expected, as shown here in Figure 1 (F. Bryan and M. Maltrud, private communication). The specific mechanism through which the jets were degraded was never identified, but replacement of the quasi-monotonic advection scheme with the original centered-in-space scheme was sufficient to recover a more realistic representation of the jets.

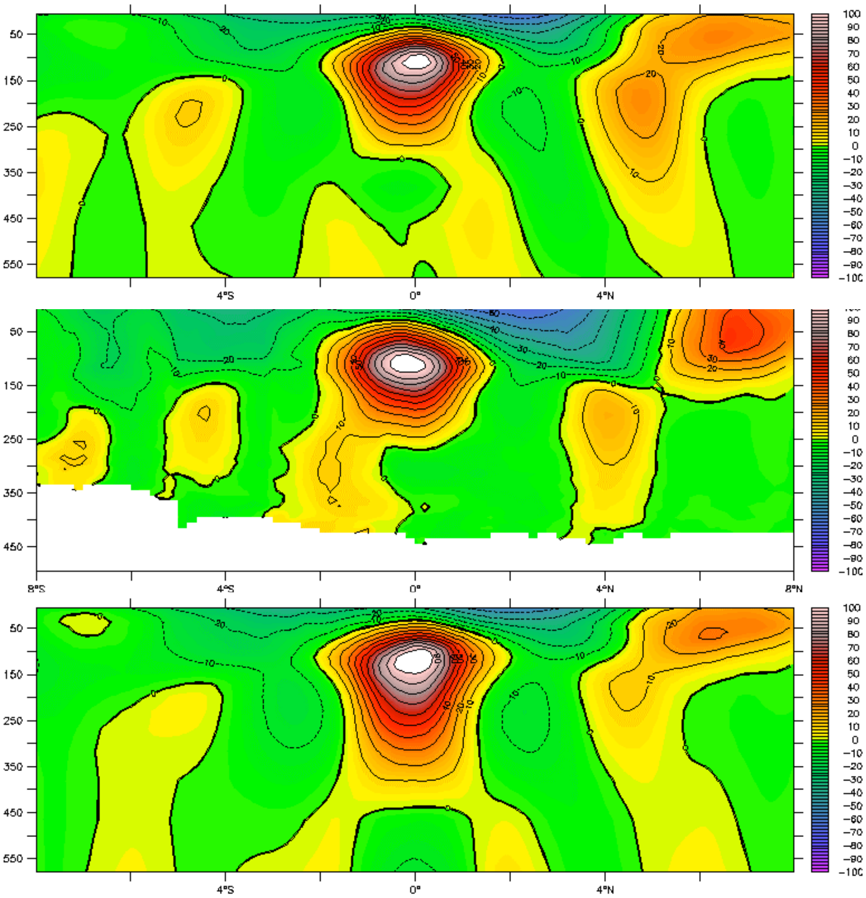

Figure 1: Equatorial Pacific velocities through an upper ocean section at 220°E,(top) from the 0.1° fully global simulation of Maltrud et al. (2010) with centered advection; (middle) from the observations of Johnson et al. (2002); and again (bottom) from the model but with the flux-limited Lax-Wendroff advection scheme of K. Lindsay (private communication). The poorer representation of the equatorial jet structure in the bottom panel, presumably due to the impact of dissipation implicit to the advection scheme, offers one illustration of why ocean modelers may be reticent to adopt alternatives to the centered scheme.

This example is offered in order to illustrate how it is that ocean modelers may still find reason to choose centered-in-space advection. The new finding we present is, however, meant to motivate the reconsideration of alternative schemes. Although ocean modelers have been willing to accept the dispersive error associated with centered advection as the lesser of perceived evils, these errors may not be limited to the generation of isolated, local blemishes, but may instead represent a leading source of spurious cooling.

2. Problematic Results from a Simple Model Configuration

The problem we take up here arose in a simple reentrant zonal channel with a sill, presented in Hecht et al. (2008) in order to evaluate their implementation of the LANS-α turbulence parameterization (Foias et al. (2001)) in the Los Alamos Parallel Ocean Program (Smith et al. (1992), Dukowicz and Smith (1994), Smith and Gent (2002)), an ocean general circulation model based on the primitive equations. Here, we do not consider results from this newer turbulence parameterization, but instead consider the problematic results which arise with use of the well-established Gent-McWilliams parameterization of isopycnal tracer mixing (referred to hereafter as GM; see Gent and McWilliams (1990), Danabasoglu et al. (1994) and Gent et al. (1995)).

The reentrant channel is an idealized representation of the Southern Ocean, as shown in Figure 2. The forcing of the model consists of a zonal wind stress and a simple heat flux based on restoring to the temperature profile indicated in the figure. It is relevant to note that the coldest temperature to which the model sea surface temperature is nudged is 2°C.

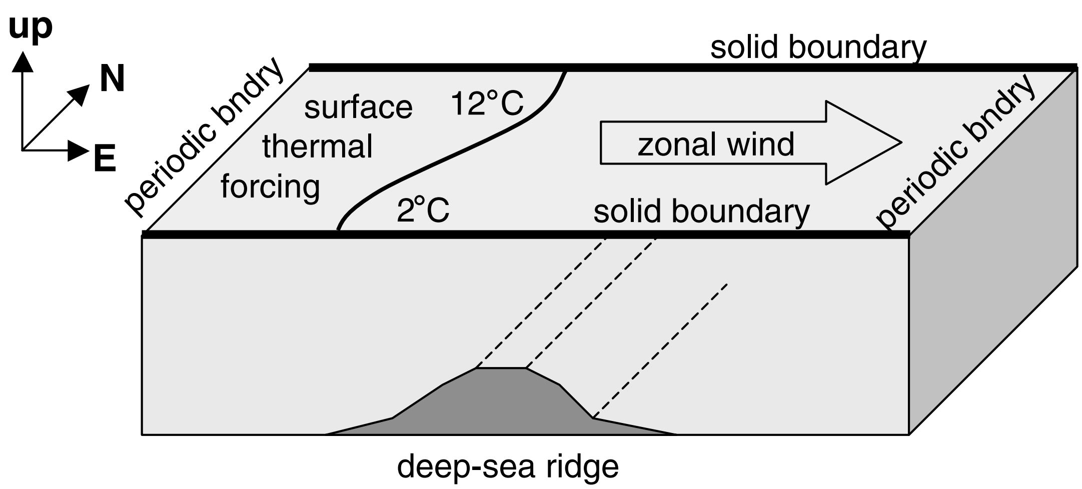

Figure 2: Channel model configuration, as used in and reprinted from Hecht et al. (2008). The zonally-reentrant domain is centered about 60°S. Thermodynamic forcing is thermal only, in the form of a restoring (with time constant of 150 days over 50 meters) to a target temperature varying from 2 to 12°C. Under this forcing, any temperatures of less than 2°C must be spurious.

The model domain spans 16° in latitude, centered about 60°S, and for computational efficiency the flow is reentrant after only 32° of longitude. In all of the cases shown here the model resolution is 0.4° in latitude and 0.8° in longitude, providing a nearly uniform aspect ratio in terms of zonal to meridional grid spacings. The implementation of GM isopycnal tracer mixing we use is based on the more efficient "skew-flux" form introduced in Griffies (1998), and is limited to isopycnal slopes less than 1%. Other relevant parameterizations include a simple Richardson number-dependent vertical mixing scheme (Pacanowski and Philander (1981)) and convective mixing through enhanced vertical mixing in response to static instability. Initially, we use the second-order centered-in-space discretization of advection.

The problem that faces us is that of understanding an extraordinary, pathological cooling that appears when we switch from horizontal biharmonic mixing of tracers to the GM isopycnal tracer mixing parameterization. This extreme cooling is evident even in a volume-mean time series of potential temperature, as in the lower-most curve of Figure 3. The initial point on this time series is the equilibrium value produced by the model as configured in the control case of Hecht et al. (2008), with horizontal biharmonic tracer mixing.

Some degree of cooling was expected with the transition from horizontal tracer mixing to GM. Within 175 years, however, a cell appears, at depth and against the sill, which is actually colder than the coldest temperature to which the surface is nudged. It is not unknown for ocean models to produce pathologically cold temperatures if the tracer advection scheme is not monotonic. Here, however, the entire deep ocean cools to unrealistically

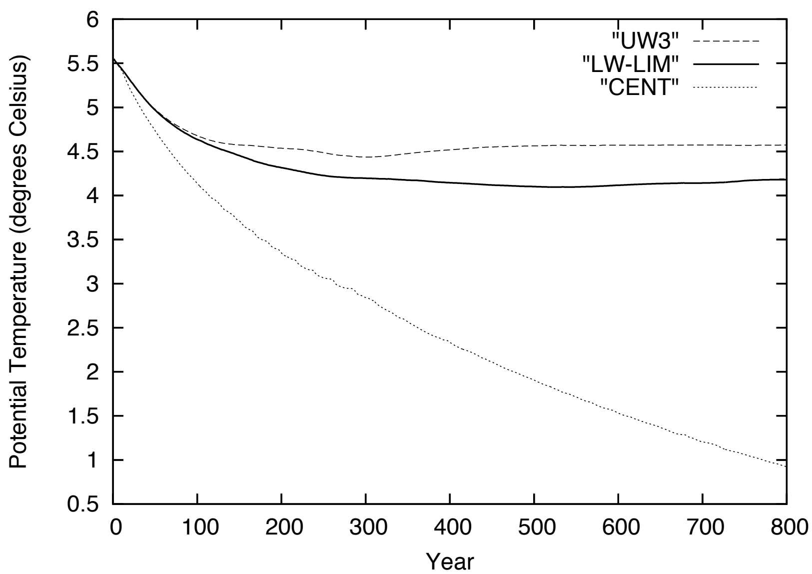

Figure 3: Volume-mean potential temperature as a function of time from integrations with three different tracer advection schemes. The lower curve was produced with centered differencing, the upper curve with the third-order upwind scheme of Holland et al. (1998), and the middle curve with the flux-limited Lax-Wendroff advection scheme of K. Lindsay (private communication). The cooling seen in the third-order upwind and flux-limited cases is due to the physical effect of parameterized eddies (the initial condition had been produced without use of the GM parameterization), whereas the spurious cooling of the centered differencing case is the subject of this paper.

cold values as the simulation is extended through a few more centuries. After approximately 425 years, the volume-mean potential temperature itself falls below the range of temperatures produced by the surface forcing.

Before going on to identify the mechanism behind this pathological cooling, we comment further on the model state. After 800 years of model integration, toward the end of the time series of Figure 3, one cell in the model domain has a temperature of less than $-1°$C, fully 3° beneath the coldest value to which the surface is nudged. In Figure 4, this cell is found to be located against the sill, nearly but not quite at the deepest model level. Waters colder than the coldest surface nudging value of 2°C fill the entire depth of the ocean below 1000 meters.

A horizontal slice at depth, containing the coldest cell, is shown in Figure 5. The strongest velocities are in the lee of sill, and the coldest cell lies at a point of convergence, where the vertical velocity is consequently determined to be upwards.

Despite the extreme cooling at depth, the surface and near-surface waters remain reasonably warm. The average surface temperature is in fact slightly warmer than in the control case of Hecht et al. (2008), and the enhanced outgoing surface heat flux allowed for by this slight increase in sea surface temperature correctly accounts for the overall domain-averaged cooling.

An inspection of advective and diffusive tendencies acting on the coldest cell indicates that the advective term is causing this coldest point to become colder yet (note that advection does not include a bolus velocity contribution, as we are using the skew-flux form of the tracer mixing parameterization). When we replace the centered advection with a quasi-monotonic form of the

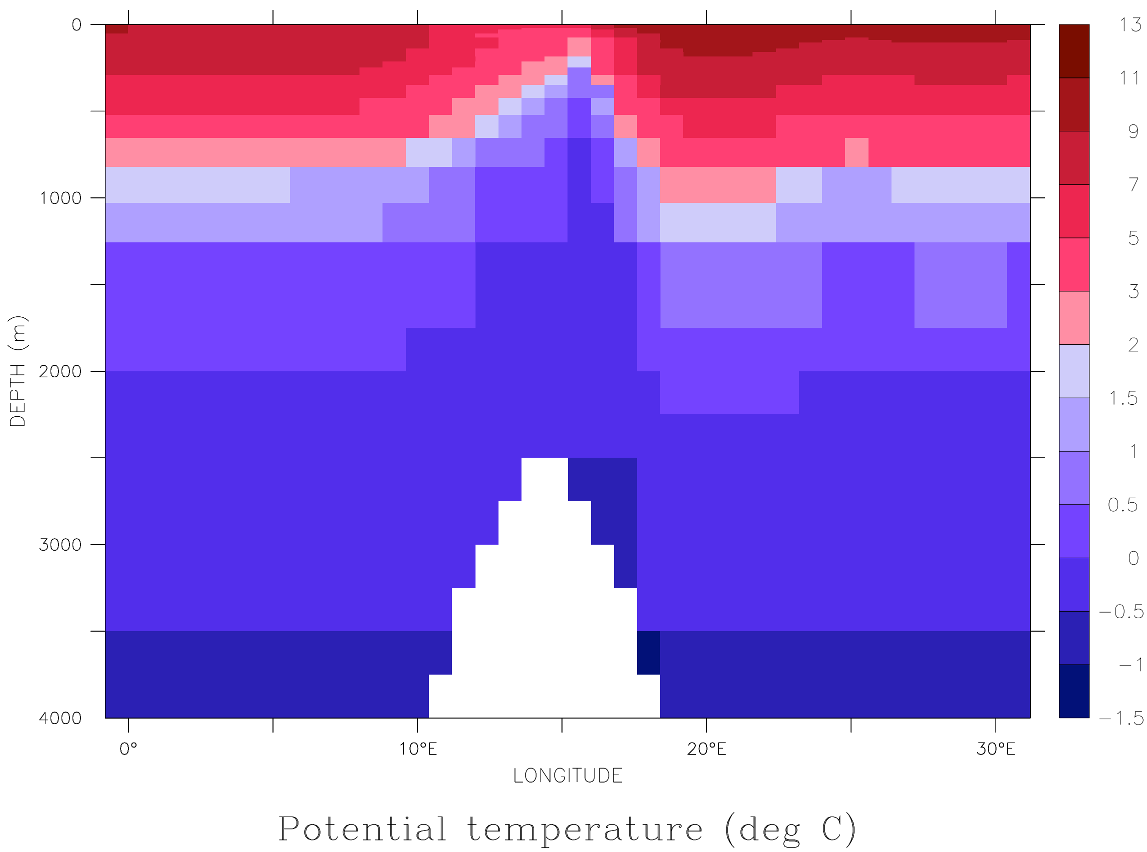

Figure 4: A zonal section of potential temperature at 55.8°S, at model year 800. One cell in the model domain has a temperature which has fallen below −1°C; this coldest cell is located one level up from the deepest model level. All waters shaded in blue have become colder than any temperature to which surface waters are nudged, and have been produced instead through dispersive numerical effects.

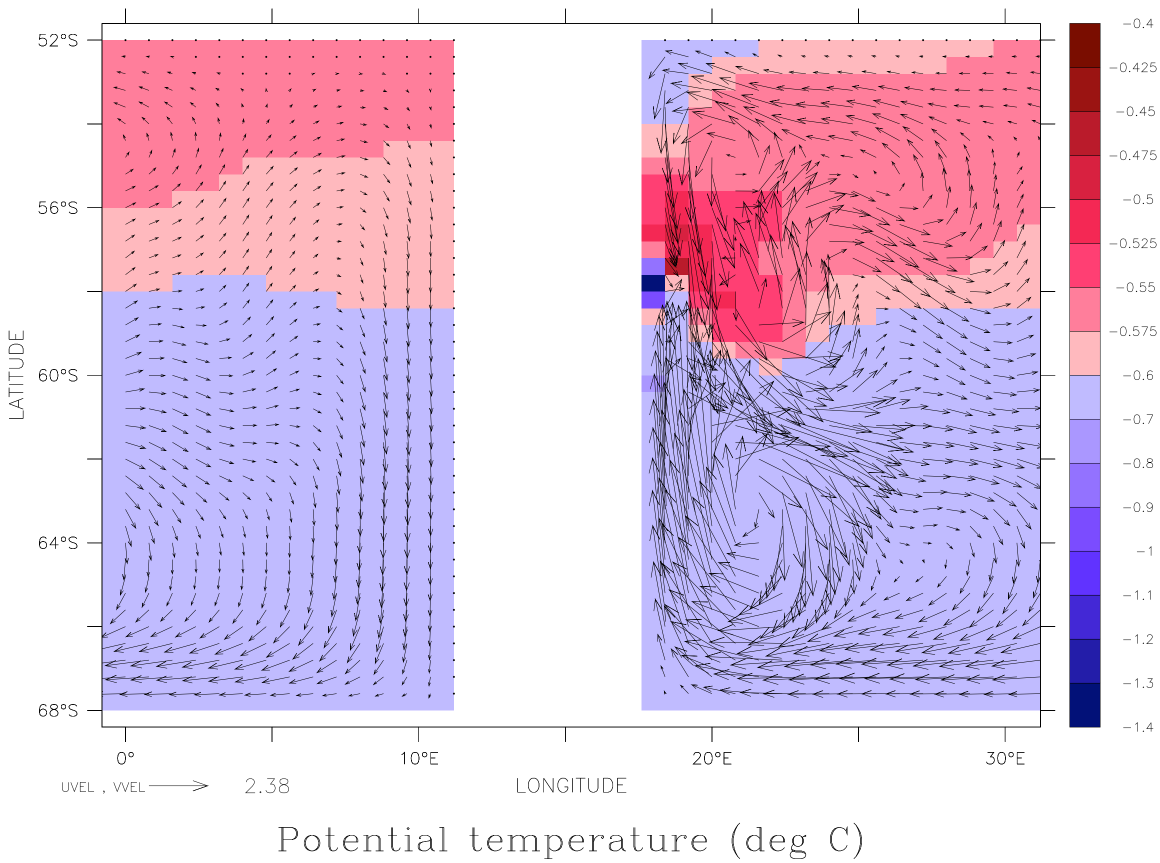

Figure 5: A horizontal section within the next-to-deepest level, centered about 3625m, and at year 800. The coldest cell is located just above the last step of the sill (as evident in the profile view of Figure 4). Velocity vectors are drawn over the potential temperature field.

Lax-Wendroff scheme (as above, K. Lindsay, private communication) and repeat the simulation, the volume mean temperature drops only modestly, as seen in the time series represented by the solid line of Figure 3. This drop in mean temperature is only what one would expect with use of GM isopycnal tracer mixing (it is the bolus velocity term, represented here through the antisymmetric component of the mixing tensor (Griffies (1998)), which tends to flatten isopycnals and causes this more moderate and physically based cooling). The potential temperatures also remain within reasonable bounds when we use the so-called third-order upwind scheme of Holland et al. (1998), as indicated by the dashed curve of Figure 3.

The vertical dependence of extreme cooling is more readily discerned in Figure 6. Level-averaged temperatures first fall below 2°C, the lower limit of the range of surface forcing, around year 200. Waters above 250m show little drift in temperature, indicating that vertical heat transports contribute little net divergence there, even if heat passes through en route to the surface, where it can be dissipated. At levels below 1000 m persistent loss of heat occurs, even as the minimum temperature of the forcing is greatly exceeded.

3. Discussion

The advective tendency, not the diffusive tendency, was identified as causing the coldest point to become colder yet. Ordinarily, a diffusive term of Laplacian form might be assumed to stay within the bounds of monotonicity, so long as a time step limit were not exceeded, but with the skew-flux form of GM departures from monotonicity may occur (Griffies et al. (1998), Griffies (1998)), and so this question of attribution to advective or diffusive tendency

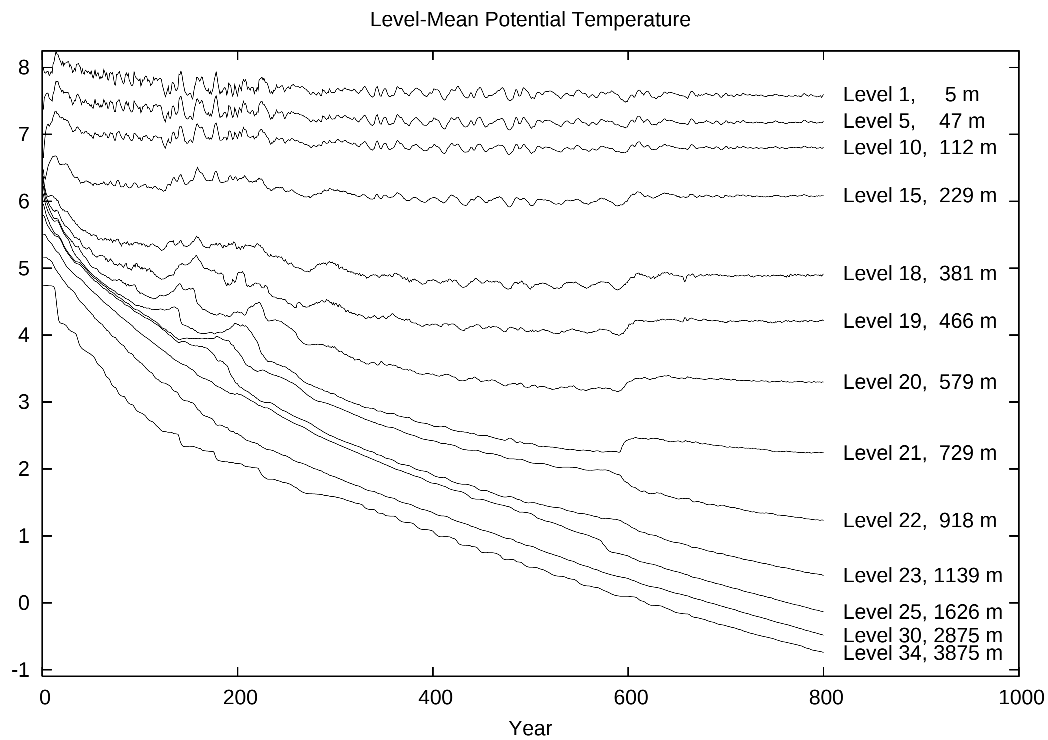

Figure 6: Level-averaged potential temperature as a function of time. Waters above 250m show little drift in potential temperature. At levels below 1000m pathological cooling occurs unabated, even after 800 years.

arose.

Colder waters at depth tend to remain at depth, and so one extremely cold cell, located at the next-to-bottom model level, will not drive the entire ocean below 1000 meters to such cold temperatures. The explanation for the larger-scale cooling of the deep ocean must address how pathologically cold waters may form at the thermocline and below, and must also explain how the surface comes to be anomalously warm, if only slightly so, allowing for a persistent enhancement of the outgoing heat flux that paces the domain-averaged cooling.

As discussed in the Introduction, the leading-order numerical error produced by the centered advection scheme is dispersive in character, rather than dissipative. This is to say that it tends to produce spurious ripples, or grid-scale noise, as opposed to spurious smoothing. The dispersive error will tend to make one cell overly warm, but only while making an adjacent cell overly cold.

It is dispersive error of just this sort that produces pairs of anomalously warm and cold waters, adjacent to one another, which may then separate in the vertical dimension under the influence of gravity, cooling the deep ocean and warming the surface. The dispersive generation of error can be expected to be largest where velocities and tracer gradients are large, in the thermocline.

If static instabilities are not mixed away but are allowed to remain, then this dispersive generation of hot and cold cells become visible. In the upper panels of Figure 7 the change in tracer concentration over a single model step is shown, with convection suppressed (the section is at the same location as that of Figure 4). The largest changes are seen not at the location of the coldest cell, at depth, but in the thermocline where velocities and tracer gradients are both high.

A measure of the vertical convective response to the sum of all other tendencies is shown in Figure 8, contoured over the same all-but-convective tendency field of the upper right-hand panel of Figure 7. Convection works to take anomalously cold waters down, and to take anomalously warm waters upwards. Each dispersively-generated source of warm water need not necessarily transport that warmth all the way to the surface in one continuous action. Collectively, the many sources of warm water contribute to produce a spurious transport of heat toward the surface. These individual sources of anomalous warmth are paired with sources of anomalously cold water, as the advection scheme is conservative. The overall process through which dispersive advective error drives the spurious upward transport of heat involves anomalously warm cells which trigger upward convection and anomalously cold cells driving downward convection, with both contributing to the spurious upward heat flux, producing ever colder deep waters.

The extreme cooling seen here is not caused by the use of GM isopycnal tracer mixing. The cooling appears because GM is not as capable of controlling the dispersive error produced by the advection scheme, as compared with the use of a simple and more spatially uniform horizontal tracer mixing. Formally, this requirement for a certain minimum level of dissipation in order to ensure the control of grid scale noise is discussed in terms of a grid-Peclet number constraint in Griffies (2004) (Peclet number being the analog of Reynolds number, but for scalar transport). The issue is illustrated by

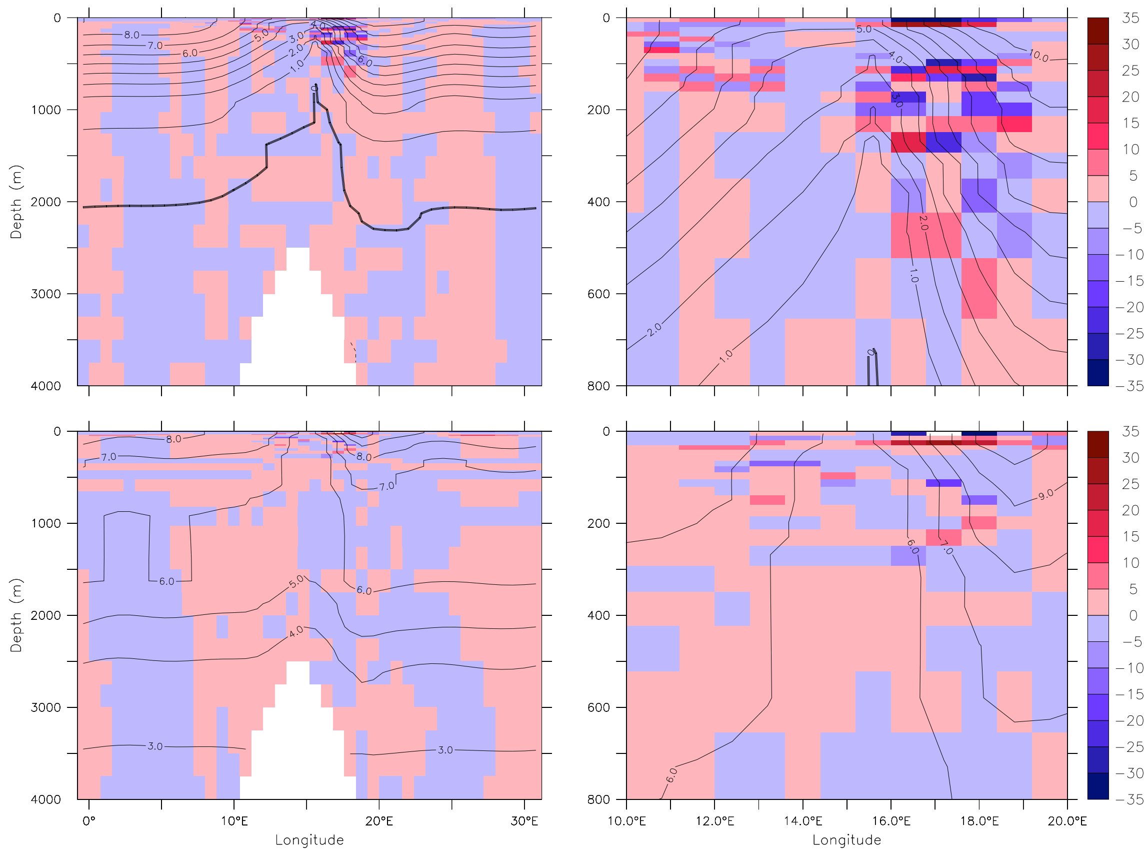

Figure 7: Temperature tendency evaluated over a model time step, with convective response to static instability suppressed for this one step (units are millikelvin per model step of 7200 seconds). The problematic case with centered differencing is shown at top, with magnified view at upper right. The section is taken at 57.8°S, the latitude at which the coldest point in the domain is found at this time of 800 years. Potential temperature is drawn over the tendency field with a contour interval of 1°C. The case produced with third-order upwinding, at bottom, exhibits far less generation of dispersive numerical error on which vertical convection might act.

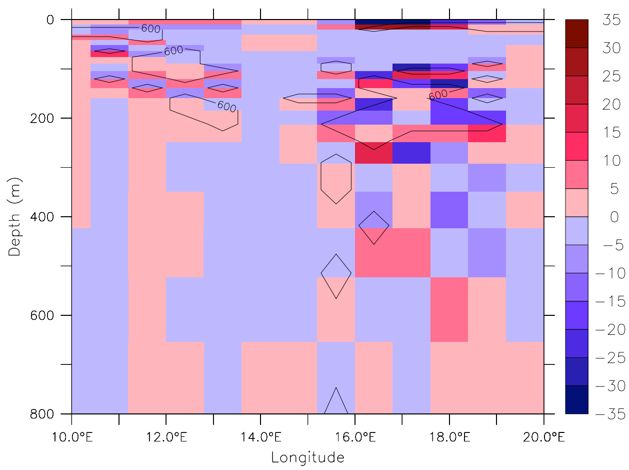

Figure 8: The same temperature tendency field as shown in the upper panels of Figure 7, but with a measure of vertical convective response to that tendency overlain. Vertically adjacent cells enclosed by contours would be subject to convective mixing, producing an upward flux of heat (mixing of warm anomalies with overlying waters, of cold anomalies with underlying waters) in response to spurious extrema produced through disperive numerical effects.

Hecht et al. (1995), where the observation is made that domain-wide control of grid scale noise may result in excessive smoothing of the transported field. The greater potential for Peclet number violation with the use of GM isopycnal tracer mixing, and the concern for "contamination" of water masses, was raised in the appendix of Hirst and McDougall (1996), where they make the point that solutions should be checked carefully for such contamination. The potential for a dispersive advection scheme to spuriously enhance the density contrast between upper ocean and abyss was commented on by Griffies et al. (2000), and here we have seen the potential magnitude of the effect. The ocean component of a newer version of a previously documented coupled climate model, the Fast Ocean Rapid Troposhere Experiment of Sinha and Smith (2002) and Smith et al. (2004), is also reportedly affected by a similar cooling at depth, apparently due to the same mechanism investigated here (A. Blaker, private communication).

The third-order upwind scheme we consider as an alternative to centered differencing is not a monotonic scheme, and may produce considerable over- or under-shoots. The upwind-biasing of the solution, however, reduces the dispersive character of the scheme. In the lower panels of Figure 7 the tendency field produced with the third-order upwind case is shown, again with convective response to static instability suppressed. The dispersive production of warm and cold cells is much reduced, relative to what is seen in the problematic centered differencing case, and the spurious vertical transport and secular cooling of the intermediate and deep ocean is consequently much reduced.

There is one aspect of our problem which presents an extreme challenge to the use of GM isopycnal mixing with a noisy advection scheme. With uniform salinity, as in this problem, isopycnal surfaces are coincident with isothermal surfaces, and the Redi component of GM can do little to control noise. When a weak variability in salinity is introduced, however, our result still holds. For instance, with an overall variability of 0.1 ppt the spurious cooling is very nearly unaffected. One does see a significant reduction in the overall cooling rate when a more typical oceanic variability of 1.0 ppt is specified, and yet one can be assured that pairs of anomalously warm and cold cells are still being created at every time step by the dispersive advection scheme, even if the Redi diffusion is now able to lessen the impact of the dispersive error over much of the domain.

4. Conclusion

The results shown here were produced in an idealized context, with simple forcing and topography, and yet the conditions responsible for the persistent accumulation of error are found in ocean climate models. In those places in which velocities and thermal gradients are high and the salinity gradient is weak one must expect a spurious upward heat flux to occur, so long as a highly dispersive advection scheme is used along with isopycnal tracer mixing. It may be difficult in the more realistic context to identify the extent to which dispersive error biases the water properties in an ocean climate model, where deficiencies in surface forcing and large scale circulation must also be considered, and where numerical error may not necessarily drive a water mass beyond obvious physical bounds, but such errors must be expected to bias sub-thermocline waters towards colder temperatures.

One hazard incurred with use of upwind-weighted advection schemes is well known to ocean modelers. Under the Veronis Effect spurious diapycnal mixing across a front presents a sort of short-circuit to the large-scale heat transport (Veronis (1975), Böning et al. (1995)). Less well understood issues such as that illustrated in Figure 1 also present a concern regarding use of schemes with leading-order numerical error of dissipative form. Here we have shown that dispersive error, or the rippling produced by a spatially-centered advection scheme, cannot be dismissed as a merely cosmetic concern, but may also introduce a significant bias, in this case toward a colder ocean below the thermocline. Hirst and McDougall (1996) called for careful inspection of solutions to identify this sort of numerical contamination of water masses. We call for the prudent elimination of the source of numerical contamination represented by the use of second-order centered-in-space advection.

A numerical error which violates the second law of thermodynamics in such a persistent way, through creation of spurious dispersive warm and cold extrema which then drive a secular cooling, is a particularly damaging type of error. Nevertheless, one should not simply trade the hazards of one error for those of another, and so a renewed effort must be mounted to gain confidence in the use of better tracer advection schemes in ocean modelling so as to minimize the spurious cross-frontal mixing associated with dissipative error while also eliminating the spurious cooling that is a consequence of uncontrolled dispersive error.

5. Acknowledgments

We thank Mathew Maltrud and Frank Bryan for the result shown in Figure 1 and Gokhan Danabasoglu for comments on the manuscript. The ideas presented here were developed in conversation with the other ocean modelers at Los Alamos. This work was supported by the Department of Energy's Office of Science. Los Alamos National Laboratory is operated by Los Alamos National Security, LLC for the Department of Energy.

References

Adcroft, A., Campin, J., Heimbach, P., Hill, C., Marshall, J., 2005. MIT-gcm manual. Technical Report. MIT. http://mitgcm.org/pelican/online_documents/manual.html.

Böning, C.W., Holland, W.R., Bryan, F.O., Danabasoglu, G., McWilliams, J.C., 1995. An overlooked problem in model simulations of the thermohaline circulation and heat-transport in the Atlantic Ocean. J. Clim. 8, 515 – 523.

Bryan, K., 1969. A numerical method for the study of the circulation of the World Ocean. J. Comput. Phys. 4, 347—376.

Danabasoglu, G., McWilliams, J.C., Gent, P.R., 1994. The role of mesoscale tracer transports in the global ocean circulation. Science 264, 1123–1126.

Dukowicz, J.K., Smith, R.D., 1994. Implicit free-surface method for the Bryan-Cox-Semtner ocean model. J. Geophys. Res. 99, 7,991—8,014.

Foias, C., Holm, D.D., Titi, E.S., 2001. The Navier-Stokes-alpha model of fluid turbulence. Physica D: Nonlinear Phenomena 152-153, 505 – 19.

Gent, P.R., McWilliams, J.C., 1990. Isopycnal mixing in ocean circulation models. J. Phys. Oceanogr. 20, 150—155.

Gent, P.R., Willebrand, J., McDougall, T.J., McWilliams, J.C., 1995. Parameterizing eddy-induced tracer transports in ocean circulation models. J. Phys. Oceanogr. 25, 463–474.

Gerdes, R., Koberle, C., Willebrand, J., 1991. The influence of numerical advection schemes on the results of ocean general circulation models. Clim. Dyn. 5, 211—226.

Griffies, S., 1998. The Gent-McWilliams skew-flux. J. Phys. Oceanogr. 28, 831–841.

Griffies, S., Pacanowski, R., Hallberg, R., 2000. Spurious diapycnal mixing associated with advection in a z-coordinate ocean model. Mon. Weather Rev. 128, 538–564.

Griffies, S.M., 2004. Fundamentals of Ocean Climate Models. Princeton University Press.

Griffies, S.M., Gnanadesikan, A., Pacanowski, R.C., Larichev, V.D., Dukowicz, J.K., Smith, R.D., 1998. Isoneutral diffusion in a z-coordinate ocean model. J. Phys. Oceanogr. 28, 805 – 30.

Griffies, S.M., Harrison, M.J., Pacanowski, R.C., Hallberg, R.W., 2004. A technical guide to MOM4. GFDL Ocean Group Technical Report

5. NOAA/Geophysical Fluid Dynamics Laboratory. Available on-line at http://www.gfdl.noaa.gov/˜fms.

Hecht, M.W., 2006. Forward-in-time upwind-weighted methods in ocean modelling. Int. J. Numer. Meth. Fl. 50, 1159–1173.

Hecht, M.W., Holland, W.R., Rasch, P.J., 1995. Upwind-weighted advection schemes for ocean tracer transport: An evaluation in a passive tracer context. J. Geophys. Res. 100, 20763—20778.

Hecht, M.W., Holm, D.D., Petersen, M.R., Wingate, B.A., 2008. Implementation of the LANS-alpha turbulence model in a primitive equation ocean model. J. Comput. Phys. 227, 5691–5716.

Hecht, M.W., Wingate, B.A., Kassis, P., 2000. A better, more discriminating test problem for ocean tracer transport. Ocean Modelling 2, 1–15.

Hirst, A., McDougall, T., 1996. Deep-water properties and surface buoyancy flux as simulated by a z-coordinate model including eddy-induced advection. J. Phys. Oceanogr. 26, 13201343.

Holland, W.R., Bryan, F.O., Chow, J.C., 1998. Application of a third-order upwind scheme in the NCAR Ocean Model. J. Clim. 11, 1487—1493.

Johnson, G.C., Sloyan, B.M., Kessler, W.S., McTaggart, K.E., 2002. Direct measurements of upper ocean currents and water properties across the tropical Pacific during the 1990's. Prog. Oceanogr. 52, 31–36.

Maltrud, M., Bryan, F., Peacock, S., 2010. Boundary impulse response functions in a century-long eddying global ocean simulation. Environmental Fluid Mechanics 10, 275–295.

Pacanowski, R., Philander, S., 1981. Parameterization of vertical mixing in numerical models of tropical oceans. J. Phys. Oceanogr. 11, 1443–1451.

Sinha, B., Smith, R., 2002. Development of a fast Coupled General Circulation Model (FORTE) for climate studies, implemented using the OASIS coupler. Internal Document 81. Southampton Oceanography Centre. 67pp.

Smith, R.D., Dukowicz, J.K., Malone, R.C., 1992. Parallel ocean general circulation modeling. Physica D: Nonlinear Phenomena 60, 38—61.

Smith, R.D., Gent, P., 2002. Reference manual of the Parallel Ocean Program (POP). Los Alamos National Laboratory report LA-UR-02-2484. Los Alamos National Laboratory. Los Alamos, NM.

Smith, R.S., Dubois, C., Marotzke, J., 2004. Ocean circulation and climate in an idealised Pangean OAGCM. Geophys. Res. Lett. 31, L18207.

Veronis, G., 1975. in Numerical Models of Ocean Circulation. Natl. Acad. Sci., Washington, D.C. The role of models in tracer studies. pp. 133–146.